Environ Geol (2008) 54:9–22
DOI 10.1007/s00254-007-0788-5

ORIGINAL ARTICLE

Extraction of potential debris source areas by logistic regression technique: a case study from Barla, Besparmak and Kapi mountains (NW Taurids, Turkey)

M. C. Tunusluoglu · C. Gokceoglu · H. A. Nefeslioglu · H. Sonmez

Received: 20 October 2006 / Accepted: 30 April 2007 / Published online: 1 June 2007

Abstract Debris flow is one of the most destructive mass movements. Sometimes regional debris flow susceptibility or hazard assessments can be more difficult than the other mass movements. Determination of debris accumulation zones and debris source areas, which is one of the most crucial stages in debris flow investigations, can be too difficult because of morphological restrictions. The main goal of the present study is to extract debris source areas by logistic regression analyses based on the data from the slopes of the Barla, Besparmak and Kapi Mountains in the SW part of the Taurids Mountain belt of Turkey, where formation of debris material are clearly evident and common. In this study, in order to achieve this goal, extensive field observations to identify the areal extent of debris source areas and debris material, air-photo studies to determine the debris source areas and also desk studies including Geographical Information System (GIS) applications and statistical assessments were performed. To justify the training data used in logistic regression analyses as representative, a random sampling procedure was applied. By using the results of the logistic regression analysis, the debris source area probability map of the region is produced. However, according to the field experiences of the authors, the produced map yielded over-predicted results. The main source of the over-prediction is structural relation between the bedding planes and slope aspects on the basis of the field observations, for the generation of debris, the dip of the bedding planes must be taken into consideration regarding the slope face. In order to eliminate this problem, in this study, an approach has been developed using probability distribution of the aspect values. With the application of structural adjustment, the final adjusted debris source area probability map is obtained for the study area. The field observations revealed that the actual debris source areas in the field coincide with the areas having high probability values on this final map.

Keywords Debris · NW Taurids · GIS · Logistic regression · Limestone · Probability map

M. C. Tunusluoglu · C. Gokceoglu (✉) · H. Sonmez
Department of Geological Engineering, Applied Geology Division, Hacettepe University, Beytepe, 06532 Ankara, Turkey
e-mail: cgokce@hacettepe.edu.tr

H. A. Nefeslioglu
Department of Geological Research, General Directorate of Mineral Research and Exploration, 06520 Ankara, Turkey

Introduction

The northern slopes of the Barla-Besparmak and Kapi mountains of the Taurids mountain belt at western part of the Mediterranean Region of Turkey present a highly steep gradient. In this region, there exists an important amount of debris deposit in both channels at upper elevations and foot zones of the mountain slopes. The debris materials in the channels at upper elevations can be triggered by heavy rainfalls and result in some catastrophic debris flows. In general, the wide interest in researches on Quaternary deposits of west-central Anatolia is due to the existence of many populated areas and mountain resorts to which slope avalanches pose a serious hazard (Nemec and Kazanci 1999). Although it is possible to find a number of recent publications on the various aspects of debris flow hazard (e.g., Rickenmann 1999; Ishikawa et al. 2003; Jomelli et al. 2004; May and Greswell 2004; Scally and Owens 2004;

Malet et al. 2004, 2005; Garcin et al. 2005; Wen and Aydin 2005; Glade 2005; Jakob 2005; Chien-Yuan et al. 2005), there is no study in literature on the assessment of debris source areas, except the study performed by Crowley et al. (2003). In the study performed by Crowley et al. (2003), potential debris flow source areas on Mount Shasta (California, USA) were analyzed employing airborne and satellite remote sensing data. A complete determination of debris source areas by both field investigations and air-photo interpretations are sometimes highly difficult due to the fact that mountainous regions generally have extremely steep slopes, and scale of air-photos does not allow carrying out such studies. When working in large areas, a full debris source area mapping is almost impossible by both field and air-photo studies. However, it is possible to prepare a debris source area inventory by these methods and this inventory provides a basis to other mapping approaches such as statistical analyses. Determination of debris source area has crucial importance for debris flow hazard assessments because areal extent and volume of debris materials, which are the major components of these assessments are directly controlled by the areal distribution of these source areas. For this reason, the main goals of the present study are to prepare an inventory map of the debris source locations of the study area, and to apply logistic regression technique for prediction of possible debris source locations. For the purpose, the study is composed of three main stages: (a) extensive field observations to identify the areal extent of debris source areas, (b) air-photo studies to determine the debris source areas, and (c) desk studies including adaptation of the data into a Geographical Information System (GIS) environment and statistical assessments.

Characteristics of the study area

The study area is located at the connection point of West Taurids and Middle Taurids (Fig. 1). This region is also called as Lakes Region or the Isparta Triangle. Isparta Triangle is bounded by Antalya Gulf, and three lakes namely Burdur, Hoyran and Beysehir Lakes. This region is composed of different rock associations based on stratigraphical and structural properties. Considering the purpose of the study and the areal extent of the study area, in the present study, the Geyik Mountain and the Barla Mountain associations are briefly summarized in the following paragraphs.

The relatively autochthonous Geyik Mountain Unit that extends along the long axis of Taurides constitutes the base line of Central Taurides. It consists of an Infra-Cambrian, Cambrian and Ordovician basement which is transgresivelly overlain by the Upper Paleozoic, Triassic and Lower Jurassic clastics and carbonate rocks, and platform type of a thick carbonate section of Jurassic to Lower Tertiary age that is bounded by Eocene flysch (Ozgul et al. 1991).

The Barla mountain is surrounded by Senirkent plain at north, Tertiary flysch of the Senirkent sub-unit at west, Isparta plain at south and Egirdir Lake at east. The Barla Mountain, which is constituted of a number of mountains and high hills, extends in E-W direction. Length, width and height of these mountain belt are around 30 km, 10–12 km and 2,400–2,800 m, respectively.

The Barla Mountain sub-unit includes the sedimentary rock unit from the Upper Triassic to Lower Eocene. Ayazmana Formation, which is composed of sandstone and shale with reef limestone blocks, is the oldest rock unit of the Barla Mountain sub-unit, which appears as an allochthon on the Senirkent unit. Ayazmana formation is overlain by the Norian-Rhaetian dolomites (Sariyer Dere Dolomite) and Liassic limestones, which are rich in algae (Yassiviran limestone). The thickness of this formation is approximately 500 m and it includes abundant paleodasycladus (Ozgul 1976; Ozgul et al. 1991).

The Kapi Mountain limestone is represented by rudist clastic turbidicit limestone then red-beige micrite of pelagic foraminifer from base to top. The Kazan Pinari formation, which is defined in Barla Mountain sub-unit is composed of Lower Tertiary, Upper Paleogene-Lower Eocene micrite and calsiturbidite and clastic flysch facies (Ozgul et al. 1991).

The material produced on the source area surface is released as a result of gravitation, freezing and thawing, and pressure of water supplied by precipitation. For this reason, assessment of precipitation is important because it contributes to the release of material from the source area. For the assessment of precipitation data of the study area, the data provided from the Senirkent and Uluborlu Meteorology Stations located in the study area were employed. The region receives a long-term (years of 1975–2004) average annual rainfall of over 54 and 50 mm, respectively. A mass movement in the form of debris flow occurred in Senirkent town on 13 July 1995. This disaster resulted in 74 deaths , and demolition and destruction of 180 houses. Moreover, systems of communication, sewage, drinking water and electricity systems have been considerably damaged. In addition, approximately 1 year later, a new debris flow phenomenon occurred on July 18 and 19, 1996. However, due to warning of local dwellings, no loss of life occurred. When making a close inspection of precipitation data recorded at the Senirkent and Uluborlu Meteorology Stations, it is clear that the amount of the precipitation is very high (Fig. 2). In other words, the values of total monthly precipitation recorded by the Senirkent Meteorology Station in July 1995 and July 1996 are 88.8 and 73.9 mm, respectively while those recorded at the

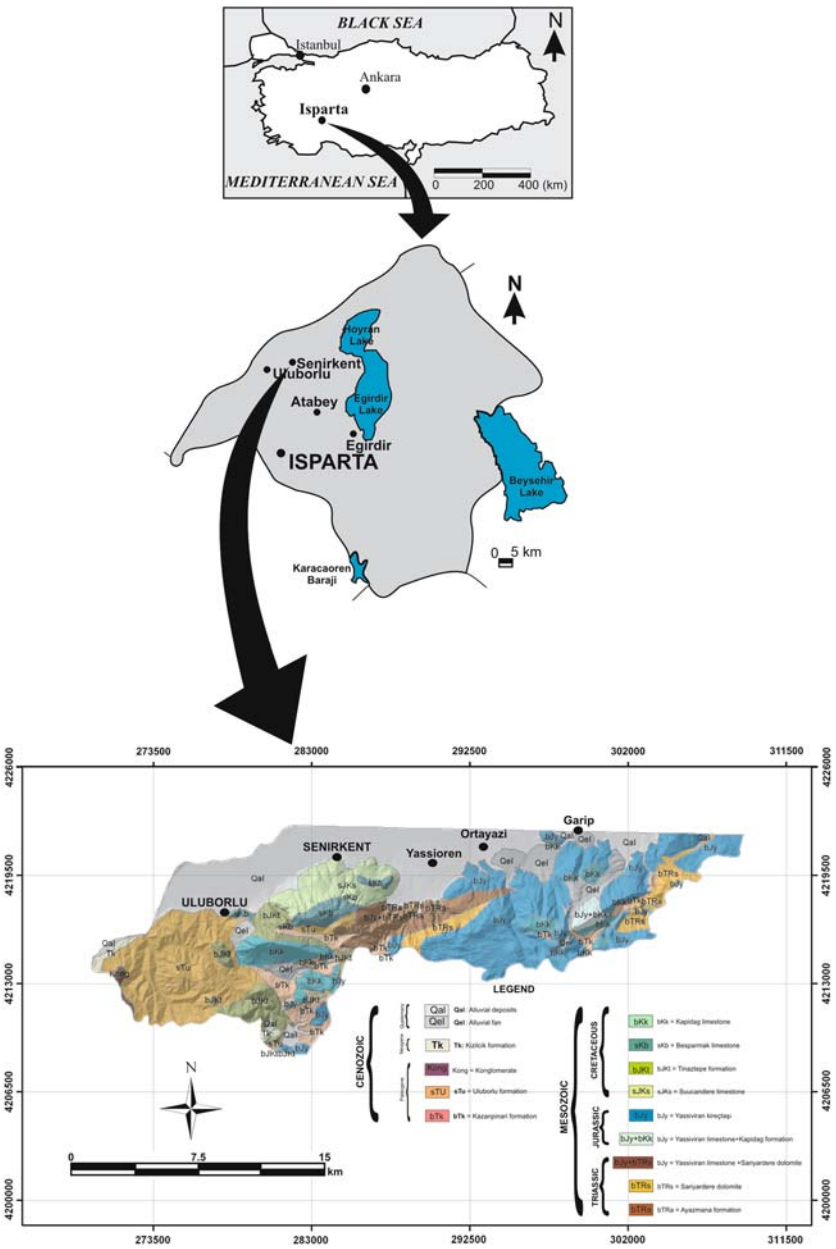

Fig. 1 Location and geological map of the study area

Uluborlu Meteorology Station are 79.6 and 105.2 mm, respectively. In the assessment of the long period average monthly precipitation values of July for Senirkent (16.6 mm) and Uluborlu (21.8 mm), these precipitations occurred in July 1995 and July 1996 can be considered as a meteorological anomaly. These assessments show that some heavy rainfalls triggering the accumulated debris material can occur in the study area.

Air-photo interpretations

The study area exhibits mainly high altitudes and steep slopes. This character does not allow easy access to each spot in the area for field observation. For this reason, an extensive air-photo interpretation was carried out to extract the possible debris source areas using vertical black and white aerial photographs of medium scale (1:35,000), dated in 1956 and 1991. In the study area, the debris material is produced by various outcropping limestones. The results of the debris source area inventory study are given in Table 1. The Kapidag limestone, Kazanpinarı formation, Suucandere limestone, Bespar-mak limestone, Tinaztepe formation, Yassiviran lime-stone+Kapidag formation and Uluborlu formation have debris production potential (Table 1). However, in order to make an objective assessment for debris production potential of the lithological units, the following debris

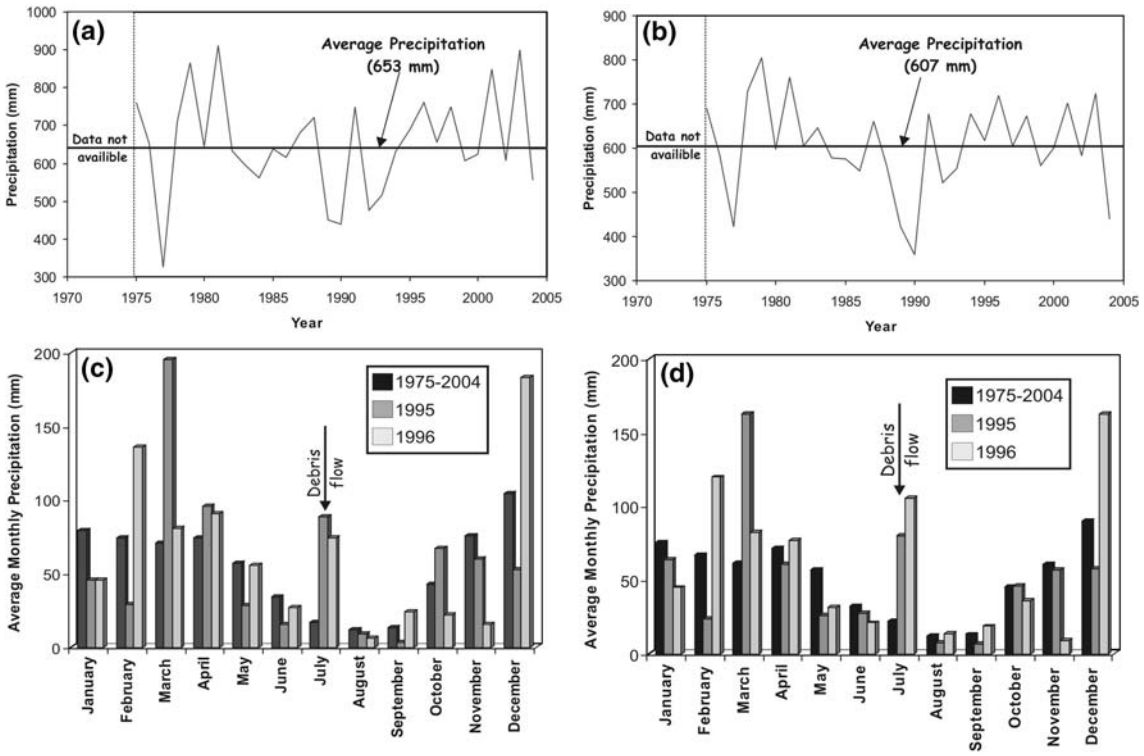

Fig. 2 Variation of annual precipitation values recorded in Senirkent (**a**) and Uluborlu (**b**) meteorology stations; *histograms* showing long-term (1975–2004, 1995 and 1996) monthly precipitation values of Senirkent (**c**) and Uluborlu (**d**)

Table 1 Lithological distribution on whole area and on debris source area inventory

Lithology	Symbol	On whole study area		On debris source area inventory		Debris source intensity
		Frequency (no. of pixels)	%	Frequency (no. of pixels)	%	
Kapidag limestone	BKk	26,054	5.66	1,434	14.23	0.06
Kazanpinari fm.	BTk	22,639	4.92	27	0.27	0.00
Suucandere limestone	SJKs	25,034	5.44	1,071	10.63	0.04
Besparmak limestone	SKb	8,028	1.74	1,799	17.86	0.22
Kizilcik fm.	Tk	2,990	0.65	0	0.00	0.00
Tinaztepe fm.	BJKt	19,534	4.24	3,663	36.34	0.19
Yassiviran limestone	BJy	101,876	22.12	996	9.88	0.01
Yassiviran limestone + Kapidag fm. (not distinguished)	bJy_bKk	4,330	0.94	627	6.22	0.14
Yassiviran limestone + Kapidag fm. (not distinguished)	bJy_bTRs	22,514	4.89	0	0.00	0.00
Ayazmana fm.	bTRa	635	0.14	0	0.00	0.00
Sariyardere dolomite	bTRs	17,464	3.79	0	0.00	0.00
Konglomera	Kong	1,354	0.29	0	0.00	0.00
Alluvium	Qal	111,972	24.32	0	0.00	0.00
Cemented debris	Qel	22,977	4.99	436	4.33	0.02
Uluborlu fm.	sTu	73,059	15.87	24	0.24	0.00

source intensity index (Eq. 1) is suggested. The debris source intensity of any lithology (DSI_i) is ratio of the number of pixels including debris source area of any lithology (lithology-i) ($NPDS_i$) to the total number of pixels of the lithology-i in the whole study area (AL_i).

$$DSI_i = \frac{NPDS_i}{AL_i} \quad (1)$$

Where, DSI_i is the debris source intensity of lithology-i. $NPDS_i$ is the number of pixels including debris source area of lithology-i and AL_i is the total area of lithology-i in the whole study area.

When making a close inspection of Table 1, it is possible to say that the Besparmak limestone (0.22), the Tinaztepe formation (0.19) and the Kapidag formation (0.14) have the highest debris material production capacity, among the lithological units in the study area.

No vegetation cover is observed when the altitude is approximately higher than 2,200 m. In other words, the study area with an altitude value of 2,200 m or more is barren. This allows extracting possible debris source areas with the aid of the air-photo interpretations. The major problem is the scale of air-photos and it is almost impossible to identify small source areas from the air-photo studies. The large areas, however, were easily identified and a debris source area inventory map was drawn (Fig. 3). When identifying the debris source areas by air-photo studies, some visual criteria are used. If a debris accumulation is detected in the channels and relatively flat areas at the footzone of a barren slope, this slope is accepted as a debris source area. Following debris flow channels, some additional source areas without debris material accumulation in the channels and relatively flat areas at the footzone are determined.

Field investigations

In the second stage of the study, an extensive field investigation was performed to check the findings obtained from air-photo interpretations and to understand the mechanisms of debris generation. The boundaries determined by air-photo interpretations were checked by field investigations and necessary corrections were done in the field at accessible locations. At not only higher elevations but also lower elevations, the debris generation is observed. This is perhaps one of the most important observations. However, this situation was not determined by air-photo interpretations due to vegetation cover at lower altitudes. The main source of the debris in the study area is the Besparmak limestone. It can be stated that there is a major structural control on the debris generation. If the dip directions of slopes and bedding planes are parallel or nearly parallel to each other, no debris generation is observed. Dip of the bedding planes must be towards the slope face for generation of debris (Fig. 4). This situation results in a difficulty when preparing debris source area probability map because there is a major structural control on generation of debris, and this control should be considered. In the latter parts of the present paper, an approach will be given to overcome this difficulty. When applying the field studies, in addition to debris source areas, some observations on the main characteristics of the debris material are also observed. The main observation was carried out on the grain size of the debris material. No change was observed on the grain size of debris material depending on the altitude. This indicates that transportation of debris material is provided by debris flows. In other words, there is no other transportation mechanism except for debris flow. In addition, the debris material occurs not only at higher altitudes but also at lower altitudes in the study area. On the basis of field observations, it can be concluded that the debris material is generally deposited in the channels and mountain slopes with lower slope angles (lower than 15°). The debris materials deposited in such zones can reach considerable volumes and transform into catastrophic debris flows depending on some triggering factors such as earthquake or

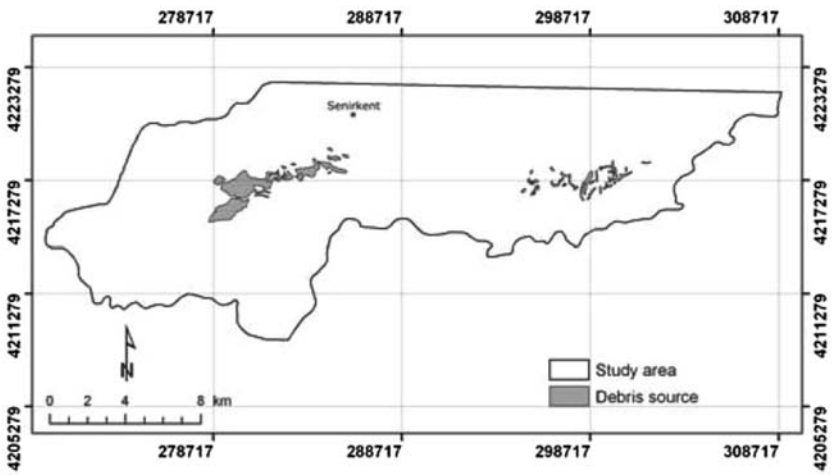

Fig. 3 Debris source area inventory map of the study area

Fig. 4 Structural control on the debris generation; dip of the bedding planes are into the slope face

heavy precipitation etc. It should be noted that the mapping and/or extraction of debris material distribution in the study area are beyond the purposes of this study. Instead, digging out the source areas generating these debris material accumulations constitutes the primary aim of this scientific research paper.

Production of index maps

To assess debris source areas and to produce index maps, some of topographical parameters such as elevation, slope, aspect, plan curvature, profile curvature, stream power index (SPI), and sediment transport capacity index (LS) were employed. All the analyses related to these terrain factors were performed in ArcView 3.2 GIS environment. For the purpose, terrain-mapping unit was selected as grid cells (pixels). Spatial resolution of the study area was set to $25 \times 25 m^2$. The maps of all index parameters given above were derived from a digital elevation model (DEM) produced by digitizing 10 m altitude contours of the 1/25,000 scaled topographical maps of the study area. The topographic elevations vary between 925 and 2,800 m in the region (Fig. 5a). Simple descriptive statistical evaluations of each parameter were performed into two groups: (a) pixels representing debris source areas and (b) pixels representing free from debris source areas. The descriptive statistics of topographical parameters are of great importance in order to the morphological conditions of debris generation locations in the study area. In addition, frequency-distribution patterns are also crucial for the assessments of these topographical properties. For this reason, in addition to descriptive statistics of these factors, their frequency distributions are also provided in this section.

While the distribution of the topographic elevations free from debris source areas shows a similarity with the distribution of topographic elevations of whole area, the distribution of the pixels representing debris source area is quite different (Fig. 6). This is a normal situation because the debris source areas are generally located at upper elevations. One of the most important topographical parameters governing the production of debris material is slope. Debris material mostly occurs at talus slopes. A talus slope can be described as an accumulation of rock debris at the base of a steep mountain slope and these steep mountain slopes generally constitute the main source of debris generation. Considering this simple evaluation, theoretically it could be expected that most of debris source area should have high gradient values in the region. To investigate this estimation, a slope map of the study area given in Fig. 5b is produced. The slope angle values of the pixels representing debris source areas vary from 5° to 65° while their average is about 36° (Table 2). The average value of slope angle of the pixels free from debris source areas is, however, 16° (Table 2). This shows that the hypothesis established above could be adequate and the slope angle is one of the most representative topographical indicators for the assessment of debris source areas in the study area. The other DEM-derived parameter employed in the study is aspect (Fig. 5c). Majority of the slopes free from debris source area in the area face north and limited number of pixels represent south-facing slopes (Fig. 6). The aspect map representing debris source areas has no south-facing slope. This indicates that the aspect is one of the main topographical attributes influencing the generation of debris material, as well.

Slope curvatures were also investigated in order to evaluate their effects on generation of debris material. The term curvature is generally defined as the curvature of a line formed by intersection of a random plane with the terrain surface (Wilson and Gallant 2000). The curvature value can be evaluated calculating the reciprocal value of the radius of curvature of the line. Hence, while the curvature values of broad curves are small, the tight ones have higher values. Slope curvature values were calculated using a script namely DEMAT (Digital Elevation Model Analysis Tool) compiled in the Avenue soft computing language of ArcView GIS by Behrens (2005). While the positive values of slope curvature define the convexity, the negative ones present the concavity of the terrain surface. Plan curvature (Fig. 5d) is described as the curvature of a contour line formed by intersection of a horizontal plane with the surface. The influence of plan curvature on the erosion processes is the convergence or divergence of water during downhill flow. This parameter constitutes one of the main factors controlling the geometry of the debris generation zones. This can be easily seen if the mean plan

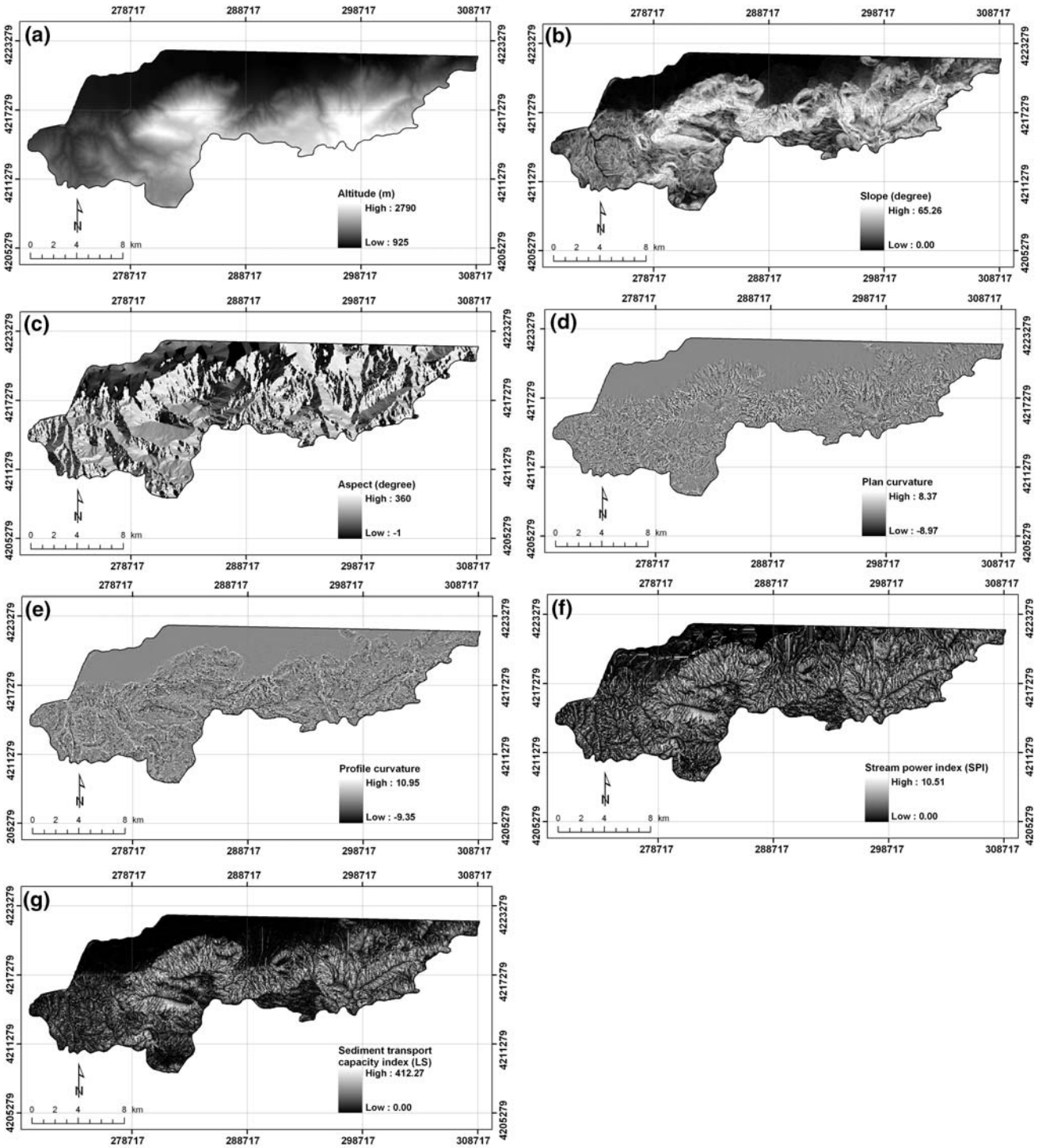

Fig. 5 Altitude (**a**), slope (**b**), aspect (**c**), plan curvature (**d**), profile curvature (**e**), stream power index (**f**) and sediment transport capacity index (**g**) maps of the study area

curvature values of the pixels representing debris source areas (0.05) are compared with pixels representing free from debris source areas (0.01) (Table 2). The profile curvature (Fig. 5e) is the curvature in the vertical plane parallel to the slope direction. It measures the rate of change of slope and therefore influences the flow velocity of water draining the surface and thus erosion and the resulting downslope movement of sediment. While the values of minimum and maximum profile curvatures of debris source areas and the areas free from debris are

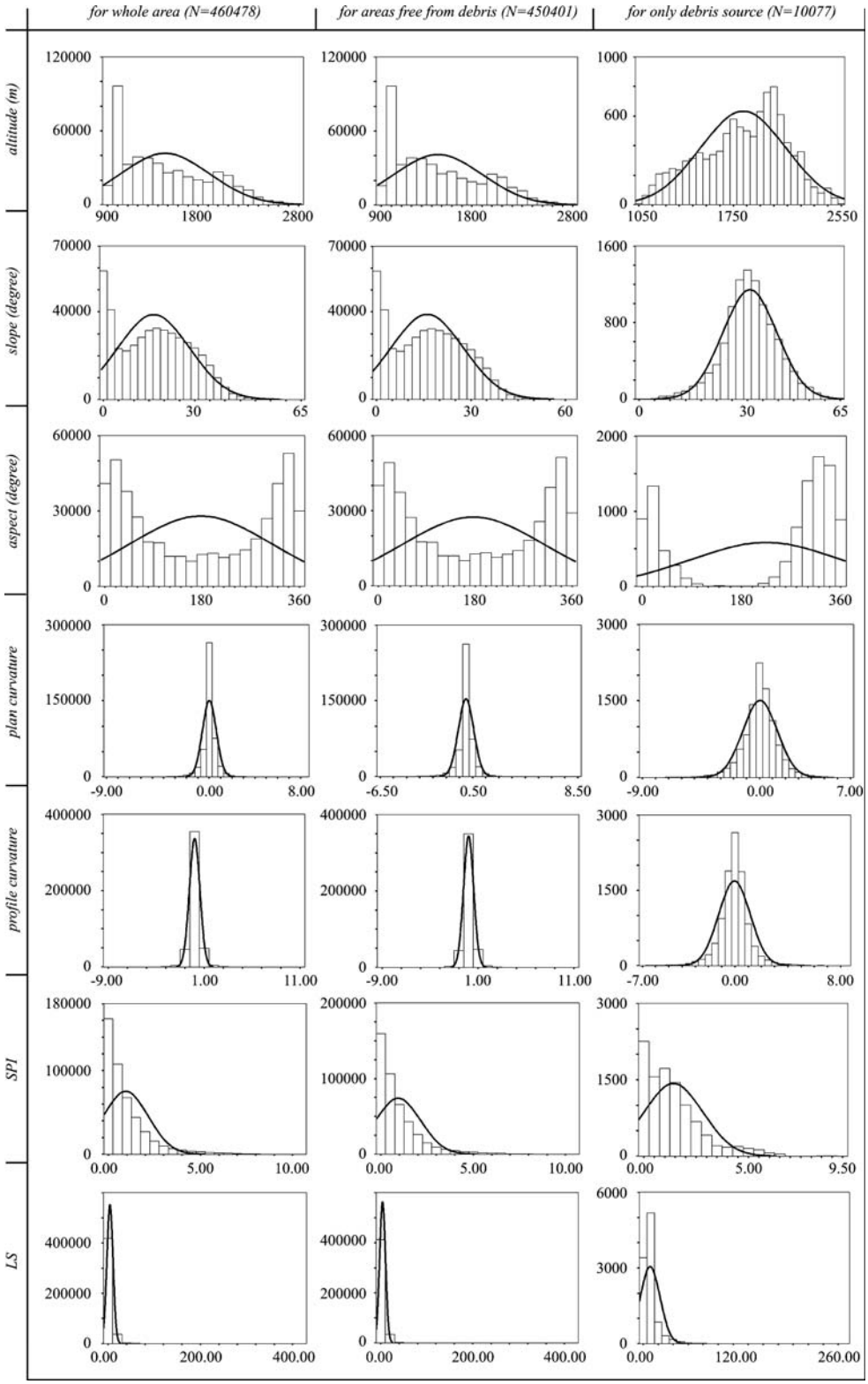

Fig. 6 Frequency distributions of the DEM derivative parameters

–7.08, 8.42, and –9.35, 10.95, respectively, the mean profile curvature values are 0.01 for debris source area and –0.04 for the areas free from debris (Table 2). These simple descriptive statistical evaluations suggest that the profile curvature parameter also strictly controls the zones of debris generation.

Primary topographical attributes such as slope, aspect, and slope curvatures are calculated directly from the

Table 2 Descriptive statistics of continuous parameters

Data	Variable	Min.	Max.	Mean	Mode	Median	Variance	Std. Deviation	Skewness	Kurtosis
For whole area (N = 460,478)	Altitude (m)	925.00	2790.00	1471.71	950.00	1375.15	193250.52	439.60	0.57	–0.78
	Slope (degree)	0.00	65.26	16.51	0.00	16.28	140.21	11.84	0.28	–0.82
	Aspect (degree)	–1.00	360.00	177.40	–1.00	177.83	17210.86	131.19	0.01	–1.64
	Plan curvature	–8.97	8.37	0.01	0.00	0.00	0.37	0.61	–0.59	9.77
	Profile curvature	–9.35	10.95	0.01	0.00	0.00	0.30	0.55	0.27	12.96
	SPI	0.00	10.51	0.94	0.00	0.52	1.49	1.22	2.29	6.64
	LS	0.00	412.27	3.97	0.00	2.11	44.21	6.65	8.28	199.16
For areas free from source (N = 450,401)	Altitude (m)	925.00	2790.00	1463.85	950.00	1363.44	192498.40	438.75	0.61	–0.74
	Slope (degree)	0.00	62.28	16.08	0.00	15.91	133.12	11.54	0.26	–0.91
	Aspect (degree)	–1.00	360.00	176.34	–1.00	174.80	17121.20	130.85	0.03	–1.64
	Plan curvature	–6.73	8.37	0.01	0.00	0.00	0.34	0.58	–0.63	8.90
	Profile curvature	–9.35	10.95	0.01	0.00	0.00	0.27	0.52	0.32	11.27
	SPI	0.00	10.51	0.93	0.00	0.51	1.47	1.21	2.31	6.81
	LS	0.00	412.27	3.85	0.00	2.04	40.67	6.38	7.85	189.13
For only debris source areas (N = 10,077)	Altitude (m)	1063.45	2540.00	1823.21	1500.00	1860.35	100557.15	317.11	–0.31	–0.65
	Slope (degree)	0.00	65.26	35.79	36.17	35.74	77.13	8.78	–0.18	0.65
	Aspect (degree)	–1.00	359.98	224.68	313.92	299.72	18934.43	137.60	–0.74	–1.31
	Plan curvature	–8.97	7.06	0.05	0.00	0.07	1.78	1.33	–0.28	3.09
	Profile curvature	–7.08	8.42	–0.04	–0.03	–0.03	1.42	1.19	0.07	5.59
	SPI	0.00	9.41	1.42	0.00	1.10	1.98	1.41	1.51	2.77
	LS	0.00	267.34	9.38	0.00	6.98	172.92	13.15	7.91	113.52

derivatives of a topographic surface (Wilson and Gallant 2000). On the other hand, the secondary topographical attributes are computed from two or more primary attributes. According to Wilson and Gallant (2000), the majority of these secondary attributes comes from the ability of describing patterns as a function of process. In this study, two well-known secondary topographical attributes were also evaluated. One of the secondary topographical attributes used in this study is SPI (Fig. 5f). It is a measure of erosive power of water flow based on assumption that discharge (q) is proportional to specific catchment area (A_s) (Eq. 2) (Moore et al. 1991).

$$\mathrm{SPI} = A_s \tan\beta \tag{2}$$

where, A_s is the specific catchment area (m^2m^{-1}), β is the slope gradient in degree. The index, SPI, is one of the main factors controlling the water erosion. The water erosion contributing to earth surface process can be considered as one of the components of the generation of debris material. Descriptive statistical evaluations (Table 2) suggest that the importance of the index SPI in generation of debris material is comprehensible because there is considerable difference between the mean values of SPI for debris source areas (1.42) and for areas free from debris (0.93).

The other secondary topographical attribute used in this study is the sediment transport capacity index (LS) (Moore and Burch 1986) (Fig. 5g). The calculation of LS value is given in the equation below:

$$\mathrm{LS} = (m + 1)(A_s/22.13)^m(\sin\beta / 0.0896)^n \tag{3}$$

where, A_s is the specific catchment area (m^2m^{-1}), β is the slope gradient (in degrees), values of m and n are 0.4 and 1.3, respectively (Moore and Wilson 1992). This parameter was derived from unit stream power theory and is equivalent to the length–slope factor in the revised universal soil loss equation in certain circumstances, where slope length <100 m and slope < 14° (Wilson and Gallant 2000). However, these conditions could not be satisfied in this study due to the morphological characteristics of the study area. The mean values of LS of debris source areas and areas free from debris are 9.4 and 3.85, respectively (Table 2). These results also evidently indicate that LS is a useful parameter in differentiating debris sources.

Application of logistic regression technique

In engineering geology and geomorphology literature, the logistic regression technique is widely used in producing

regional landslide susceptibility maps (Bernknopf et al. 1988; Jade and Sarkar 1993; Wieczorek et al. 1996; Atkinson and Massari 1998; Gorsevski et al. 2000; Lee and Min 2001; Dai et al. 2001; Dai and Lee 2002, 2003; Ohlmacher and Davis 2003; Lee 2004; Ayalew and Yamagishi 2005; Can et al. 2005), because landslide susceptibility evaluation involves a high level of uncertainty due to data limitation and model shortcomings (Zezere 2002). Besides the mapping of landslide susceptibility, some other applications of this technique could also be encountered in recent literature. The research by Brenning and Trombotto (2006) can be shown as an example. The researchers present the ability to model rock glacier and glacier distribution using logistic regression technique. In the present study, the possibility of the extraction of potential debris source areas using this approach is investigated. For this purpose, a series of logistic regression analyses were carried out to produce the debris source area probability map of the region. The fundamental principle of logistic regression is based on the analysis of a problem in which a result measured with dichotomous variables (such as 0 and 1 or true and false) is determined from one or more independent factors (Menard 1995). Generally, logistic regression involves fitting the dependent variable by using an equation in the following form:

$$Y = \text{logit}(P) = \ln[p/(1 - p)] = \beta_0 + \beta_1 x_1 + \ldots\ldots\ldots\ldots + \beta_n x_n \quad (4)$$

where p is the probability that the dependent variable (Y) is 1, $p/(1 - p)$ is the so-called odds or likelihood ratio, β_0 is the intercept, and β_1, β_2,..., β_n are coefficients that measure the contribution of independent factors (X_1, X_2,..., X_n) to the variations in Y.

The first stage in the application of logistic regression analysis is the production of data matrix. While each row data represents an individual case expressed using a terrain-mapping unit (grid cell), columnar data show the independent and dependent variables in the data matrix. It is commonly desired that all continuous variables have the same scale in multivariate statistical analysis. For this reason, continuous variables (altitude, slope, aspect, plan curvature, profile curvature, SPI, and LS) were normalized in the range of [0, 1]. Since the parameter geology is a categorical data, it was expressed in binary format with respect to each lithological definition. By considering 7 continuous variables and 15 lithological units in binary format, total 22 independent variables were included in the logistic regression analysis (Table 3). Dependent variable of the analysis is also expressed in binary format with respect to the presence (1) and absence (0) of debris source area. One of the main requests of the multivariable statistical applications is the equal sampling strategy for the training data set. This means that the ratio of presence (1)/absence (0) should be equal to 1 in the training data set. In order to ensure the training data set used in logistic regression analysis as representative, a random-sampling procedure was applied. For this purpose, five different training data sets were constructed at random. Besides, 10% of the present data (selected randomly) in each training set were excluded from the analyses as checking data sets. Thus, while whole data matrix includes 460,478 cases, the training and checking data sets contain 18,138 and 1,008 cases, respectively. By using the training data sets, ordinary logistic regression analyses were carried out to calculate the probability values, which indicate the probability of being a debris source area. All independent variables are allowed to be included in the regression equations in the ordinary method of logistic regression. They were performed iteratively within a 95 % confidence interval. In addition, classification cut-off values were **selected as 0.5 and maximum iterations were set to 12. As results of the ordinary logistic regression analyses, overall corrected percentage values for training datasets were calculated in the range of 93.8 and 94.3% (Table 4).

Table 3 List of variables used in logistic regression analysis

Variables			
Lithology		Digital elevation model (DEM)	
Name	Symbol	Name	Symbol
Kapidag limestone	bKk	Altitude	n_altitude
Kazanpinari fm.	bTk	Slope	n_slope
Suucandere limestone	sJKs	Aspect	n_aspect
Besparmak limestone	sKb	Plan curvature	n_plncurv
Kizilcik fm.	Tk	Profile curvature	n_prfcurv
Tinaztepe fm.	bJKt	Stream power index	n_spi
Yassiviran limestone	bJy	Sediment transport capacity index	n_ls
Yassiviran limestone + Kapidag fm. (not distinguished)	bJy_bKk		
Yassiviran limestone + Kapidag fm. (not distinguished)	bJy_bTRs		
Ayazmana fm.	bTRa		
Sariyardere dolomite	bTRs		
Konglomera	Kong		
Alluvium	Qal		
Cemented debris	Qel		
Uluborlu fm.	sTu		

In addition to the correct percentage values, area under curve (AUC) (Lee 2005) values were obtained between 0.961 and 0.965 from the receiver-operating characteristic (ROC) plots of the training datasets (Fig. 7). To evaluate the prediction capacities of the models constructed using different random samplings, root mean square error (RMSE) values for the checking datasets were also calculated (Table 4). RMSE values range between 0.213 and 0.241. As a consequence, according to the performance values of the training datasets and the prediction capacity values with respect to checking data sets, it could readily realized that the training data sets are evidently representative for the study area because the values given in Table 4 are very close to each other. To produce the debris source area probability map of the region the results obtained from the model having the best prediction capacity with respect to RMSE analyses of the checking data sets were considered. Eight lithological units and six topographical attributes were found as meaningful when the significance level of 0.05 is selected (Table 5). By considering the Wald test statistical values, Besparmak limestone (sKb) and Tinaztepe formation (bJKt) are the most important lithological units while slope, altitude and profile curvature are the crucial attributes with respect to generation of debris material (Table 5). Prime attention should be paid to the fact that the sign ''–'' in front of β coefficients in Table 5 has a meaning of decreasing in the possibility of being a debris source, and for the sign ''+'', vice versa. The lithologies Kizilcik formation (Tk), Yassiviran limestone + Kapidag formation (bJy_bTRs), Ayazmana formation (bTRa), Sariyardere dolomite (bTRs) and conglomerates (Kong) have high values of $-\beta$ (Table 5). This is an expected result, because the debris source intensity values of these lithologies are zero. This means that these lithologies have not been producing any debris material. For this reason, although the significances of these lithologies are too small, it was decided that they be used in the logistic regression equation. By applying Eq. 4 with β coefficients in Table 5 to the whole data set (460,478 cases), the map of potential debris source areas is obtained (Fig. 8).

However, the produced map (Fig. 8) yielded over-predicted results. As mentioned previously, this means that if slope aspect and orientation of bedding planes are same in the region, no debris generation is observed. For this reason, a structural adjustment for the map of potential debris source area is needed. Since it was observed that all debris generation occurs on the geomorphologic units of questas, it can be considered that all debris source areas mapped during field studies coincided with the geomorphologic units of questas. Consequently, this situation constitutes the main assumption of the approach proposed for the structural adjustment for the probability map of potential debris source area in this study. The second assumption is that theoretical probability distribution of slope aspect values of debris source areas is equal to the theoretical probability distribution of being a questa in the field. If P_q is the probability of being a questa, $1 - P_q$ is the probability of not being a questa. To calculate the adjusted probability (P'_d) of being a debris source area at a point in the field, $1 - P_q$ (the probability of not being a questa) is subtracted from the probability (P_d) value of being a debris source area. Calculation of the value ''$1 - P_q$'' (the probability of not being a questa) has three main stages. The first stage is the construction of the theoretical probability distribution of slope aspect values of debris source areas (Fig. 6). However, due to the categorical nature of slope aspect values, a transformation is needed to obtain the continuous slope aspect distribution. For example, value of –1 in the slope aspect values does not

Table 4 Validation assessments with respect to different random samplings

Random samplings	Correct (1) % for train data	AUC for train data	RMSE for check data
rnd-1	93.8	0.961	0.221
rnd-2	94.1	0.962	0.239
rnd-3	94.2	0.964	0.240
rnd-4	94.3	0.965	0.241
rnd-5	94.2	0.963	0.213

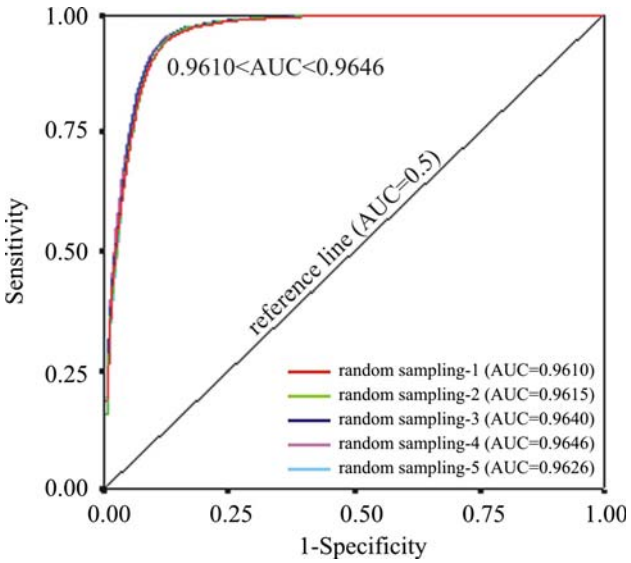

Fig. 7 Receiver operating characteristic curve and AUC evaluation with respect to different random samplings

Table 5 A coefficients and test statistics of variables in the equation

Variable	β	Std. error	Wald	Degrees of freedom	Significance	exp(β)
Lithology						
bKk	2.655	0.232	130.658	1	0.000	14.231
bTk	–0.105	0.315	0.111	1	0.740	0.900
sJKs	2.297	0.233	96.811	1	0.000	9.943
sKb	4.849	0.243	397.475	1	0.000	127.645
Tk	–15.187	4667.649	0.000	1	0.997	0.000
bJKt	4.674	0.230	412.653	1	0.000	107.158
bJy	1.071	0.231	21.495	1	0.000	2.919
bJy_bKk	3.245	0.265	150.121	1	0.000	25.655
bJy_bTRs	–19.042	1730.661	0.000	1	0.991	0.000
bTRa	–18.783	9845.277	0.000	1	0.998	0.000
bTRs	–18.800	1927.934	0.000	1	0.992	0.000
Kong	–16.396	8647.120	0.000	1	0.998	0.000
Qal	2.559	0.320	63.860	1	0.000	12.918
Qel	4.094	0.242	285.192	1	0.000	59.987
Digital elevation model (DEM)						
n_altitude	3.308	0.171	375.425	1	0.000	27.318
n_slope	11.123	0.251	1957.542	1	0.000	67720.548
n_aspect	0.252	0.078	10.286	1	0.001	1.286
n_plncurv	1.148	0.658	3.042	1	0.081	3.153
n_prfcurv	–3.294	0.784	17.662	1	0.000	0.037
n_spi	–0.437	0.667	0.430	1	0.512	0.646
n_ls	12.287	4.066	9.134	1	0.003	2.17E+05
Constant	–8.045	0.643	156.505	1	0.000	0.000

mean orientation information. It means the flat areas in the field. Hence, this value should be excluded from the distribution. In addition, the value ‘‘0’’ and the value ‘‘360’’ in the slope aspect distribution are equal with respect to orientation information. So, the transition from ‘‘0’’ to ‘‘360’’ should be removed (second stage). For this purpose, the slope aspect values in the range of [0, 157] were summed with the value 360. The new distribution, which shows almost an ideal theoretical normal distribution (Fig. 9) is obtained in the range of [165, 514]. The mean and the standard deviation values of this distribution are 337.32 and 42.59, respectively. As a result, the probability density function of this distribution can be written as follows.

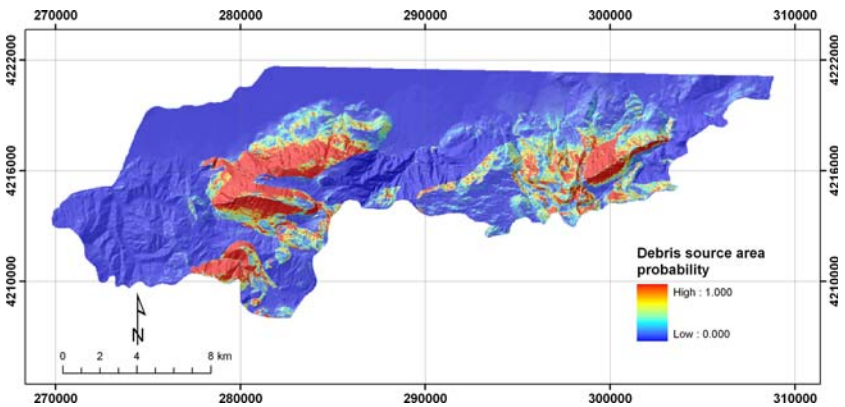

Fig. 8 Debris source area probability map of the study area

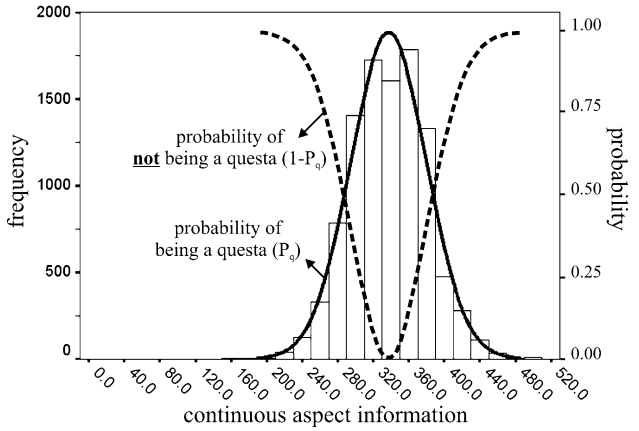

Fig. 9 The probabilistic approach for the structural adjustment

$$f(x) = [1/42.59\sqrt{(2\,\pi\,)}]\exp(-[1/(3628.04)(x\,-\,337.32)^2]) \quad (5)$$

For the last stage, using Eq. 5, the probability values of being a questa were calculated (the value ''P_q''). Then, to obtain the probability values of not being a questa, these ''P_q'' values were subtracted from 1. Thus, in order to calculate the adjusted probability (P'_d) values of being a debris source area, the values ''1–P_q'' were subtracted from the probability values of debris source areas. Finally, the adjusted potential debris source area map is obtained (Fig. 10) by using the adjusted probability values. The field observations revealed that the final adjusted map exhibits a good performance, and it can be used for debris flow hazard assessments to be performed at this site in future.

Results and conclusions

The following results and conclusions can be drawn from the present study:

a) The study area has a mountainous character and intense debris flows are frequent in the region. For this reason, investigations on debris production, accumulation and flow are frequently observed in the area.

b) The topographical features of the area do not allow easy access to every spot in the area for field investigations. For this reason, an extensive air-photo interpretation was carried out to extract the debris source areas by using black and white aerial photographs. The debris material is produced by various limestones such as the Kapidag limestone, Kazanpinarı formation, Suucandere limestone, Besparmak limestone, Tinaztepe formation, Yassiviran limestone and Uluborlu formation. In this study, for an objective assessment for debris production potential of lithological units, the debris source intensity index is introduced. This index is calculated as 0.22 for the Besparmak limestone, 0.19 for the Tinaztepe formation and 0.14 for the Kapidag formation.

c) The results of the present study revealed that logistic regression technique could be used for the extraction of potential debris source areas in such kind of studies. According to the results of logistic regression analyses, the Besparmak limestone and Tinaztepe formation are the most important lithological units, and slope, altitude and profile curvature are the most important topographical parameters among the parameters employed in this study. By using the logistic regression analyses results, the debris source area probability map was produced. However, the map yielded over-predicted results due to the effect of structural control. To eliminate this problem, a probability-based approach was introduced. After application of the approach described herein, an adjusted debris source area probability map was produced for the study area.

d) The field observations suggested that the final adjusted probability map exhibits a good performance, and it can be used for debris flow hazard assessments to be performed in future.

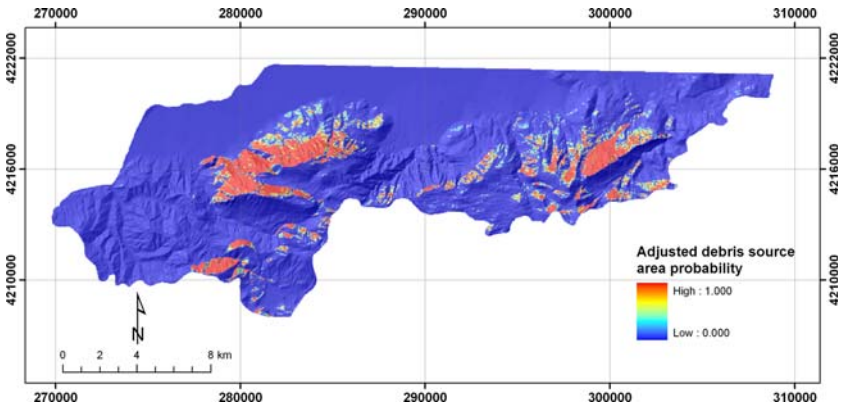

Fig. 10 Adjusted debris source area probability map of the study area

Acknowledgments This research is supported by TUBITAK (The Scientific and Technological Research Council of Turkey) with a project number of 103Y144. The authors thank Prof Dr R. Ulusay for constructive comments on the manuscript and Z.A. Erguler for his supports during the field investigations.

References

Atkinson PM, Massari R (1998) Generalized linear modelling of susceptibility to landsliding in the central Apennines, Italy. Comput Geosci 24:373–385

Ayalew L, Yamagishi H (2005) The application of GIS-based logistic regression for landslide susceptibility mapping in the Kakuda-Yahiko Mountains, central Japan. Geomorphology 65:15–31

Behrens T (2005) DEM analysis tool. http://www.arcscripts.esri.com/details.asp?dbid=10222

Bernknopf RL, Cambell RH, Brookshire DS, Shapiro CD (1988) A probabilistic approach to landslide hazard mapping in Cincinnati, Ohio, with applications for economic evaluation. Bull Int Assoc Eng Geol 25:39–56

Brenning A, Trombotto D (2006) Logistic regression modeling of rock glacier and glacier distribution: topographic and climatic controls in the semi-arid Andes. Geomorphology 81:141–154

Can T, Nefeslioglu HA, Gokceoglu C, Sonmez H, Duman TY (2005) Susceptibility assessments of shallow earthflows triggered by heavy rainfall at three catchments by logistic regression analyses. Geomorphology 72:250–271

Chien-Yuan C, Tien-Chien C, Fan-Chieh Y, Wen-Hui Y, Chun-Chieh T (2005) Rainfall duration and debris flow initiated studies for real-time monitoring. Environ Geol 47:715–724

Crowley JK, Hubbard BE, Mars JC (2003) Analysis of potential debris flow source areas on Mount Shasta, California, using airborne and satellite remote sensing data. Remote Sens Environ 87:345–358

Dai FC, Lee CF (2002) Landslide characteristics and slope instability modelling using GIS Lantau Island, Hong Kong. Geomorphology 42:213–238

Dai FC, Lee CF (2003) A spatiotemporal probabilistic modelling of storm-induced shallow landsliding using aerial photographs and logistic regression. Earth Surf Processes Landf 28:527–545

Dai FC, Lee CF, Zhang XH (2001) GIS-based geo-environmental evaluation for urban land-use planning: a case study. Eng Geol 61(4):257–271

Garcin M, Poisson B, Pouget R (2005) High rates of geomorphological processes in a tropical area: Remparts river case study (Reunion Island, Indian Ocean). Geomorphology 67:335–350

Glade T (2005) Linking debris-flow hazard assessments with geomorphology. Geomorphology 66:189–213

Gorsevski PV, Gessler P, Foltz RB (2000) Spatial prediction of landslide hazard using logistic regression and GIS. 4th international conference on integrating GIS and environmental modelling. Alberta p 9

Ishikawa Y, Kawakami S, Morimoto C, Mizuhara K (2003) Suppression of debris movement by forests and damage to forests by debris deposition. J For Res 8:37–47

Jade S, Sarkar S (1993) Statistical models for slope stability classification. Eng Geol 36:91–98

Jakob M (2005) A size classification for debris flows. Eng Geol 79:151–161

Jomelli V, Pech VP, Chochillon C, Brunstein D (2004) Geomorphic variations of debris flows and recent climatic change in the French Alps. Clim Change 64:77–102

Lee S (2004) Application of likelihood ratio and logistic regression models to landslide susceptibility mapping using GIS. Environ Manage 34:223–232

Lee S (2005) Application of logistic regression model and its validation for landslide susceptibility mapping using GIS and remote sensing data. Int J Remote Sens 26:1477–1491

Lee S, Min K (2001) Statistical analysis of landslide susceptibility at Yongin, Korea. Environ Geol 40:1095–1113

Malet JP, Maquaire O, Locat J, Remaitre A (2004) Assessing debris flow hazards associated with slow moving landslide: methodology and numerical analyses. Landslides 1:83–90

Malet JP, Laigle D, Remaitre A, Maquaire O (2005) Triggering conditions and mobility of debris flows associated to complex earthflows. Geomorphology 66:215–235

May CL, Gresswell RE (2004) Spatial and temporal patterns of debris-flow deposition in the Oregon Coast Range, USA. Geomorphology 57:135–149

Menard S (1995) Applied logistic regression analysis. Sage University paper series on quantitative applications in social sciences, vol 106. Thousand Oaks, p 98

Moore ID, Burch GJ (1986) Sediment transport capacity of sheet and rill flow: application of unit stream power theory. Water Resour Res 22:1350–1360

Moore ID, Wilson JP (1992) Length-slope factors for the revised universal soil loss equation: simplified method for estimation. J Soil Water Conserv 47:423–428

Moore ID, Grayson RB, Ladson AR (1991) Digital terrain modeling: a review of hydrological, geomorphological, and biological applications. Hydrol Processes 5:3–30

Nemec W, Kazanci N (1999) Quaternary colluvium in west-central Anatolia: sedimentary facies and paleoclimatic significance. Sedimentology 46:139–170

Ohlmacher CG, Davis CJ (2003) Using multiple regression and GIS technology to predict landslide hazard in northeast Kansas, USA. Eng Geol 69:331–343

Ozgul N (1976) Toroslarin bazi temel Jeoloji ozellikleri. Turkiye Jeooli. Kurumu Bulteni 19:65–78 (in Turkish)

Ozgul N, Bolukbasi S, Alkan H, Oztas Y, Korucu M (1991) Goller Bolgesinin Tektono-Stratigrafik Birlikleri. Ozan Sungurlu Sempozyumu Bildirileri, Ankara, 213–237s (in Turkish)

Rickenmann D (1999) Empirical relationships for debris flows. Nat Hazard 19:47–77

Scally FA, Owens IF (2004) Depositional processes and particle characteristics on fans in the Southern Alps, New Zealand. Geomorphology 69:46–56

Wen BP, Aydin A (2005) Mechanism of a rainfall-induced slide-debris flow: constrains from microstructure of its slip zone. Eng Geol 78:69–88

Wieczorek GF, Gori PL, Jager S, Kappel WM, Negussey D (1996) Assessment and management of landslide hazards near Tully Valley landslide, Syracuse, New York, USA. Proceedings of the 7th international symposium on landslides, Trondheim. Balkema, Rotterdam, pp 411–416

Wilson JP, Gallant JC (2000) Terrain analysis principles and applications. Wiley, Toronto, p 479

Zezere JL (2002) Landslide susceptibility assessment considering landslide typology. A case study in the area north of Lisbon (Portugal). Nat Hazard Earth Syst Sci 2:73–82